

Lower and Upper Critical Ordering Temperatures in Compressible Diblock Copolymer Melts from a Perturbed Hard-Sphere-Chain Equation of State

Toshiaki Hino and John M. Prausnitz*

Department of Chemical Engineering, University of California, Berkeley, and Chemical Sciences Division, Lawrence Berkeley National Laboratory, University of California, Berkeley, California 94720

Received June 2, 1997; Revised Manuscript Received February 9, 1998

ABSTRACT: The random-phase approximation is combined with the perturbed hard-sphere-chain (PHSC) equation of state for copolymer systems to represent the microphase separation transition in compressible diblock copolymer melts. The PHSC equation of state takes into account the equation-of-state effect that results from differences in compressibility between pairs of segments comprising a diblock copolymer; these differences favor demixing. Upon increasing the temperature of a microphase-separated diblock copolymer melt, theory first predicts an order-to-disorder transition that corresponds to the upper-critical-solution-temperature behavior in the binary blend of parent homopolymers. At conditions where the equation-of-state effect is significant, theory also predicts a disorder-to-order transition at further elevated temperature that follows closely the lower-critical-solution-temperature behavior in the binary blend containing the parent homopolymers. To compare theory with experiment, we obtain the binary interaction parameter between copolymer segments from the coexistence curve for the binary blend of parent homopolymers. Predicted microphase-separation-transition temperatures of diblock copolymer melts are compared with experiment for styrene-based diblock copolymer melts including poly(styrene-*block-n*-butyl methacrylate) melts that show both order-to-disorder and disorder-to-order transitions. We also discuss the pressure dependence of order-to-disorder transition temperatures of styrene-based diblock copolymer melts. Theory and experiment show semiquantitative agreement.

I. Introduction

Because of fundamental scientific interest and possible applications of block copolymers, considerable effort has been made to examine phase equilibria for block copolymer melts and those for mixtures containing block copolymers.^{1–5} A block copolymer consists of sequentially connected chemically different homopolymers. The homopolymers comprising a block copolymer are called the parent homopolymers of a block copolymer. In this work, we consider the phase behavior of a diblock copolymer melt consisting of segments A and B.

The phase behavior of an A–B diblock copolymer melt is expected to follow that of the binary blend containing parent homopolymers because both systems are characterized by the same binary interaction parameter that reflects interactions between dissimilar segments A and B. In the absence of favorable interactions such as hydrogen bonding between segments A and B, the interaction between dissimilar segments is unfavorable relative to the average of A–A and B–B interactions. Consequently, a homogeneous binary mixture of parent homopolymers exhibits upper-critical-solution-temperature (UCST) behavior upon cooling and splits into segment-A rich and segment-B rich macrophases to increase the number of contacts among similar segments.^{6,7}

Disordered diblock copolymer melts also undergo phase separation with decreasing temperature. Because of the connectivity of homopolymers comprising block copolymers, however, phase separation in diblock copolymer melts leads not to ordinary large-scale phase separation but, instead, to the formation of a variety of spatially ordered microstructures whose dimensions are comparable to the size of copolymers.^{1–5} In diblock

copolymer melts, the disorder-to-order transition upon cooling is called an upper-critical-ordering transition (UCOT).

In addition to UCST behavior, miscible polymer blends often exhibit lower-critical-solution-temperature (LCST) behavior upon heating.^{6–8} In the absence of specific interactions such as hydrogen bonding between dissimilar molecules, LCST behavior in binary polymer blends results from the equation-of-state effect, an entropic effect unfavorable to mixing. The equation-of-state effect is caused by the disparity in compressibility between the mixture's components. For polymer blends, Patterson and Robard provide a discussion on the relative importance of the equation-of-state effect and specific interactions that lead to LCST behavior.⁹

Although phase separation at elevated temperature is also expected for disordered diblock copolymer melts, the first experimental evidence of microphase separation upon heating was only recently reported by Russell et al.¹⁰ for poly(styrene-*block-n*-butyl methacrylate)^{10–12} diblock copolymer melts. This diblock copolymer also exhibits UCOT behavior. For diblock copolymer melts, the disorder-to-order transition with increasing temperature is called a lower-critical-ordering transition (LCOT).

To represent LCOT behavior in diblock copolymer melts, it is necessary to develop theories applicable to compressible diblock copolymer melts. Immediately after Russell et al.'s¹⁰ discovery of both UCOT and LCOT behaviors in poly(styrene-*block-n*-butyl methacrylate) diblock copolymer melts, Yeung et al.¹³ showed qualitatively that both UCOT and LCOT behaviors can be predicted by the random-phase approximation (RPA)^{5,14–17} for diblock copolymer melts combined with an equation-of-state theory for polymeric fluids. The

model by Yeung et al.¹³ is based on the RPA for incompressible diblock copolymer solutions developed by Fredrickson and Leibler¹⁶ that uses the Flory–Huggins lattice theory.¹⁸ In lattice theories, compressible pure fluids are modeled as incompressible binary systems where vacant lattice sites (i.e., holes) are occupied by a hypothetical component whose fraction is determined by the equation of state for the system.¹³

Similarly, prior to the experiment by Russell et al.,¹⁰ Dudowicz and Freed¹⁹ also combined the compressible RPA for diblock copolymer melts with the lattice-cluster theory that improves the Flory–Huggins lattice theory. Dudowicz and Freed¹⁹ presented a semiquantitative analysis of polystyrene/poly(vinyl methyl ether) homopolymer blends and poly(styrene-*block*-vinyl methyl ether) diblock copolymer melts. The model by Dudowicz and Freed¹⁹ predicts phase separation upon heating in both homopolymer blends and diblock copolymer melts that contain polystyrene and poly(vinyl methyl ether). Recently, Hashimoto et al.²⁰ showed some evidence of LCOT behavior in a disordered poly(styrene-*block*-vinyl methyl ether) diblock copolymer melt by small-angle neutron scattering. However, the order-to-disorder transition temperatures have not yet been measured for poly(styrene-*block*-vinyl methyl ether) diblock copolymer melts.

In this work, we present a molecular-thermodynamic model to represent both UCOT and LCOT behaviors in compressible diblock copolymer melts. Our model is similar to that of Yeung et al.¹³ because we also follow the RPA for diblock copolymer solutions presented by Fredrickson and Leibler.¹⁶ Our model, however, is different from that by Yeung et al.¹³ in calculating the interaction matrix required for the RPA. In addition, we present a more rigorous comparison of theory with experiment.

To calculate the interaction matrix, we use the recent perturbed-hard-sphere-chain (PHSC) equation of state^{21–26} that is applicable to normal fluids, nematic liquid crystals,²⁶ and polymers, including copolymers. Contrary to the other models for diblock copolymer melts,^{13,15,16,19} however, the PHSC equation of state is an equation-of-state theory in continuous space. Therefore, we first discuss our procedure to combine the RPA with the PHSC equation of state for diblock copolymer melts.

Our main objective is to represent, first, parent pure homopolymer melts; second, mixtures of parent homopolymers; and third, diblock copolymer melts using the same set of pure-component and binary parameters. We also investigate the effect of pressure on the phase behavior of diblock copolymer melts and that of mixtures containing parent homopolymers.

To present quantitative comparison of theory with experiment, we first regress the PHSC equation-of-state parameters for parent homopolymers from pressure–volume–temperature data for homopolymer melts.²⁵ The PHSC equation of state requires three parameters to represent thermodynamic properties of a homopolymer melt: segment diameter, number of segments per molecule, and the depth of the square-well potential that represents the attractive interaction on a segment basis. Next, using the PHSC equation of state for binary homopolymer blends,²⁵ one binary interaction parameter between copolymer segments is obtained from the coexistence curve for the binary blend containing parent homopolymers at ambient pressure. Finally, we predict

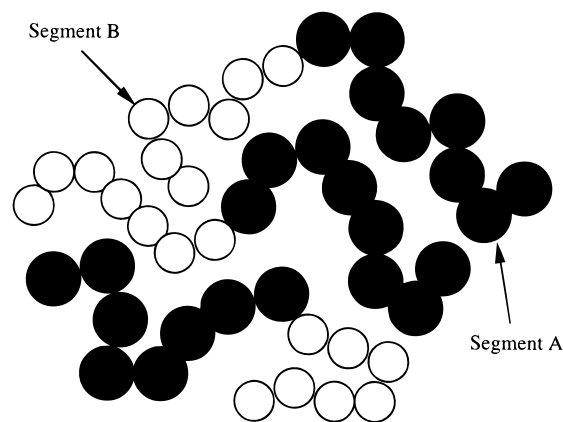


Figure 1. Schematic of a diblock copolymer melt consisting of segments A and B represented by filled and open spheres, respectively, in continuous space.

the pressure dependence of microphase-separation-transition temperatures of styrene-based diblock copolymer melts.

The present work considers only the stability of homogeneous compressible diblock copolymer melts in the weak segregation limit. Equilibrium structures of microphases are not discussed.

II. Random-Phase Approximation (RPA)

The RPA for diblock copolymer melts originally developed by Leibler¹⁵ provides a systematic procedure to calculate the Helmholtz energy density of ordered diblock copolymer melts. In this approach, the Helmholtz energy density of an ordered system is expanded around that of a disordered system in terms of the Fourier components of order parameters using the scattering functions. The scattering function matrix for real diblock copolymers consists of the scattering function matrix for ideal noninteracting Gaussian diblock chains and the interaction matrix that represents interactions among segments.¹⁵

In the RPA for diblock copolymer systems, the Flory–Huggins lattice theory¹⁸ is often used to compute the interaction matrix. In this work, however, we combine the RPA with the PHSC equation of state^{21–26} that is an off-lattice equation-of-state theory. In the PHSC equation of state, a polymer molecule is represented by a chain of tangent spheres that interact with spheres in another chain through repulsive and attractive interactions.

1. Helmholtz Energy and Stability Limit. In continuous space of volume V , we consider a diblock copolymer melt containing N molecules of type

$$(A_X B_{1-X})_r \quad (1)$$

where A and B are the segments comprising a diblock copolymer with diameters σ_A and σ_B , respectively, X is the number fraction of segment A, and r is the total number of segments per molecule. The number of segment A and that of segment B per molecule are $r_A = rX$ and $r_B = r(1-X)$, respectively. For a diblock copolymer, the numbers of $\alpha - \beta$ ($\alpha, \beta = A, B$) sequences per molecule are given by

$$r_{AA} = r_A - 1, \quad r_{BB} = r_B - 1, \quad r_{AB} = 1 \quad (2)$$

Figure 1 shows a schematic of a diblock copolymer melt in continuous space. The average packing fraction

of segment A is η_A and that of segment B is η_B ; they are given by

$$\eta_\alpha = \frac{\rho}{6} r_\alpha \pi \sigma_\alpha^3 \quad \alpha = A, B \quad (3)$$

where $\rho \equiv N/V$ is the number density. The average total packing fraction η is given by

$$\eta = \eta_A + \eta_B \quad (4)$$

We follow closely the theory for incompressible diblock copolymer solutions developed by Fredrickson and Leibler¹⁶ that uses the Flory–Huggins lattice theory. The model by Fredrickson and Leibler¹⁶ reduces to Leibler's original model for incompressible diblock copolymer melts¹⁵ by setting the number of lattice sites occupied by solvent molecules equal to zero. For a compressible melt, the lattice sites occupied by solvent molecules are replaced by vacancies. The fraction of sites that is vacant is determined by the system's equation of state.¹³

In the lattice theory of Fredrickson and Leibler,¹⁶ the average volume fraction of segment A and that of segment B are denoted as ϕ_A and ϕ_B , respectively. In the present theory, packing fractions η_A and η_B correspond to volume fractions ϕ_A and ϕ_B in ref 16. Therefore, the independent fluctuating fields in our model are $\delta\eta_A(\mathbf{x})$ and $\delta\eta_B(\mathbf{x})$ that correspond to $\delta\phi_A(\mathbf{x})$ and $\delta\phi_B(\mathbf{x})$, respectively, in ref 16. Parameters $\delta\eta_A(\mathbf{x})$ and $\delta\eta_B(\mathbf{x})$ represent the fluctuation in the packing fraction of segment A and that of segment B, respectively, at point \mathbf{x} .

We also define order parameters ψ_1 and ψ_2 by

$$\begin{pmatrix} \psi_1(\mathbf{x}) \\ \psi_2(\mathbf{x}) \end{pmatrix} = \mathbf{M} \begin{pmatrix} \langle \delta\eta_A(\mathbf{x}) \rangle \\ \langle \delta\eta_B(\mathbf{x}) \rangle \end{pmatrix} \quad (5)$$

where the angular brackets denote the thermodynamic average and

$$\mathbf{M} = \eta^{-1} \begin{pmatrix} 1 - f & -f \\ \eta & \eta \end{pmatrix} \quad (6)$$

where f is the volume fraction of segment A per chain given by

$$f = \frac{r_A \sigma_A^3}{r_A \sigma_A^3 + r_B \sigma_B^3} \quad (7)$$

Order parameter ψ_1 describes the composition fluctuation of segment A for a fixed total packing fraction. Order parameter ψ_2 represents the deviation of the total packing fraction from its average value.

In this work, we consider only the stability of homogeneous diblock copolymer melts in the weak segregation limit where the order parameters are small. In that event, it is sufficient to retain only the second-order term in the expansion of the Helmholtz energy density in the order parameters.^{13,16} The Helmholtz energy density is given by^{13,16}

$$\frac{A}{V k_B T} = \left(\frac{A}{V k_B T} \right)_{\text{dis}} + \frac{1}{2V} \sum_{ij} \int \frac{d\mathbf{q}}{(2\pi)^3} \Gamma_{ij}^{(2)}(q) \psi_i(\mathbf{q}) \psi_j(-\mathbf{q}) \quad (8)$$

where A is the Helmholtz energy, k_B is the Boltzmann constant, T is the absolute temperature, \mathbf{q} is the

scattering vector of magnitude q , $\Gamma_{ij}^{(2)}(q)$ is the second-order vertex function, and $\psi_i(\mathbf{q})$ is the Fourier transform of $\psi_i(\mathbf{x})$. The first term in the right-hand side of eq 8 is the Helmholtz energy density of a disordered system.

The matrix for the second-order vertex function is a function of \mathbf{M} given by eq 6 and the scattering-function matrix defined by¹⁶

$$\tilde{\mathbf{S}}(q) = [\eta^{-1} \mathbf{S}^{-1}(q) + \mathbf{W}]^{-1} \quad (9)$$

where \mathbf{S} is the scattering-function matrix for the non-interacting Gaussian diblock chains and \mathbf{W} is the interaction matrix defined later. These matrices are 2×2 matrixes and the indices ij ($i, j = 1, 2$) of their elements denote segment type with $i = 1$ and 2 referring to segments A and B, respectively.

The elements of matrix \mathbf{S} are functions of the modified Debye function as given by Leibler.^{15,16} Although the PHSC equation of state uses different segment diameters for chemically different segments, in calculating the scattering functions for noninteracting Gaussian diblock chains, we use the expressions for the diblock chain consisting of a uniform segment size. The elements of matrix \mathbf{S} are given by^{15,16}

$$S_{11}(q) = r v g_1(f, x) \quad (10)$$

$$S_{22}(q) = r v g_1((1 - f), x) \quad (11)$$

$$S_{12}(q) = S_{21}(q) = \frac{1}{2} r v [g_1(1, x) - g_1(f, x) - g_1((1 - f), x)] \quad (12)$$

where v is the average segment volume given by

$$v = \frac{\pi}{6r} (r_A \sigma_A^3 + r_B \sigma_B^3) \quad (13)$$

In eqs 10–12, $g_1(f, x)$ is the modified Debye function given by^{15,16}

$$g_1(f, x) = \frac{2}{x^2} [fx + \exp(-fx) - 1] \quad (14)$$

where f is the volume fraction of segment A per chain given by eq 7 and

$$x \equiv q^2 n l^2 / 6 \quad (15)$$

where n is the number of the statistical segments of (Kuhn) length l . The pair of parameters n and l models the chain statistics of a real diblock copolymer by that of an ideal Gaussian chain. Segments A and B are assumed to have the same statistical segment length. In principle, as discussed by Tanaka et al.,²⁷ a unique pair of segment diameter and statistical segment length can be assigned to each segment to compute the scattering functions for noninteracting Gaussian diblock chains. For parent polymers studied in this work, segment diameters regressed by the PHSC equation of state are close to each other. Therefore, we use the scattering functions for the diblock chain consisting of a uniform segment size. We assume that n and l are given, respectively, by r (number of segments per molecule) and the average hard-sphere diameter.

In matrix notation, the second-order vertex function is given by

$$\Gamma(q) = (\mathbf{M}^{-1})^T \tilde{\mathbf{S}}^{-1}(q) \mathbf{M}^{-1} \quad (16)$$

where matrixes \mathbf{M} and $\tilde{\mathbf{S}}$ are given by eqs 6 and 9, respectively. A disordered block copolymer melt becomes unstable against vanishingly small fluctuation in order parameters when the smallest eigenvalue of the matrix Γ becomes negative;¹³ the condition for stability of a disordered system is given in terms of the function $F(q)$ defined by¹³

$$F(q) \equiv \Gamma_{11}^{(2)} \Gamma_{22}^{(2)} - \Gamma_{12}^{(2)} \Gamma_{21}^{(2)} > 0 \quad \text{for any } q \quad (17)$$

The essential step in combining the RPA with the PHSC equation of state is the calculation of the interaction matrix \mathbf{W} in eq 9. In theories based on the Flory–Huggins lattice theory, the elements of the interaction matrix are usually obtained by solving the RPA equations as shown by Fredrickson and Leibler¹⁶ for diblock copolymer solutions. In terms of the Fourier transform, the RPA equations calculate the composition changes induced by the external potentials using the scattering functions for noninteracting Gaussian chains.

In this work, we use an alternate procedure to obtain the interaction matrix. This procedure follows a thermodynamic relation between the scattering-function matrix and the Helmholtz energy density for multicomponent systems. The derivation of the interaction matrix used here, however, is not discussed by Fredrickson and Leibler¹⁶ and by Yeung et al.¹³ for diblock copolymer solutions and melts. Therefore, we first propose a systematic procedure for computing the interaction matrix by reviewing the RPA combined with the Flory–Huggins theory for homopolymer blends and that for diblock copolymer melts.

2. Definition of the Interaction Matrix. Our approach is based on the thermodynamic relation between the Helmholtz energy density for homopolymer blends and $\tilde{\mathbf{S}}^{-1}(0)$, the inverse of the scattering-function matrix in the limit $q \rightarrow 0$. In homopolymer blends, the elements of matrix $\tilde{\mathbf{S}}^{-1}(0)$ are equal to the second derivatives of the Helmholtz energy density with respect to the segment volume fractions.²⁸

Consider first the RPA for compressible binary homopolymer blends combined with the Flory–Huggins theory.²⁸ The RPA for compressible homopolymer blends was recently discussed by Bidkar and Sanchez²⁸ using the lattice-fluid equation of state (i.e., a compressible Flory–Huggins theory). Bidkar and Sanchez,²⁸ however, did not apply their theory to compressible diblock copolymer melts. In the RPA for homopolymer blends, the scattering function matrix is also expressed by eq 9 with $\mathbf{S}(q)$ representing the scattering-function matrix for noninteracting Gaussian homopolymer chains.

In the Flory–Huggins theory for binary homopolymer blends, the Helmholtz energy consists of two contributions:²⁸ the ideal Helmholtz energy that represents the translational entropy of polymers and the nonideal Helmholtz energy that describes interactions among segments. The second derivatives of the ideal Helmholtz energy with respect to the segment volume fractions are identical to the elements of matrix $\mathbf{S}^{-1}(0)$, the inverse of the scattering-function matrix for noninteracting Gaussian homopolymer chains in the limit $q \rightarrow 0$. Therefore, by assuming that the elements of the interaction matrix \mathbf{W} are independent of q , these elements are identified as the second composition derivatives of the nonideal Helmholtz energy density.

We now consider the Flory–Huggins theory for incompressible diblock copolymer solutions developed by

Fredrickson and Leibler¹⁶ and that for compressible diblock copolymer melts by Yeung et al.¹³ In these systems, the Helmholtz energy density is also separated into the ideal and nonideal Helmholtz energies that, respectively, represent the translational entropy of diblock copolymers and interactions among segments. The nonideal Helmholtz energy density is next expressed in terms of ϕ_A and ϕ_B , the volume fraction of segment A and that of segment B, respectively.

Although not shown here, the interaction matrix derived by Fredrickson and Leibler¹⁶ and that by Yeung et al.¹³ are identical to the matrices whose elements are the second derivatives of the relevant nonideal Helmholtz energy density with respect to ϕ_A and ϕ_B . These derivatives are taken by considering ϕ_A and ϕ_B to be independent variables. On the basis of this general relationship between the interaction matrix and the nonideal Helmholtz energy density in the Flory–Huggins theory, the RPA for A–B diblock copolymer melts may also be combined with the PHSC equation of state by the following procedure.

Consistent with earlier studies, in the PHSC equation of state the Helmholtz energy density is also separated into two contributions: the ideal Helmholtz energy that is identical to the contribution from the translational entropy of polymers in the Flory–Huggins theory and the nonideal Helmholtz energy that represents interactions among segments. The nonideal Helmholtz energy is then expressed in terms of η_A and η_B by considering these variables as independent composition variables. The interaction matrix is the matrix whose elements are the second composition derivatives of the nonideal Helmholtz energy density.

3. Interaction Matrix for the PHSC Equation of State. Details of the PHSC equation of state are given in refs 21–25. In the PHSC equation of state, ΔA , the Helmholtz energy with respect to that in the standard state, is given by

$$\frac{\Delta A}{Nk_B T} = \ln(\rho k_B T) + \left(\frac{A}{Nk_B T} \right)_{\text{ref}} + \left(\frac{A}{Nk_B T} \right)_{\text{pert}} \quad (18)$$

The standard state is the ideal gas at system temperature and unit pressure. The leading term in the right-hand side of eq 18 is the configurational Helmholtz energy of an ideal gas. The terms denoted by subscripts ref and pert are the reference and perturbation terms, respectively; these terms represent repulsive and attractive interactions, respectively. The equation of state is obtained from the Helmholtz energy by

$$p = \rho^2 \left(\frac{\partial \Delta A}{\partial \rho} \right)_{T,N} \quad (19)$$

where p is the pressure.

There are two versions of the PHSC equation of state reported in the literature: the original model^{22–24} that uses a van der Waals-type perturbation term and the more recent model that uses the perturbation theory for the square-well fluid of variable well width.^{25,26} In this work, we use the latter version of the PHSC theory because that model provides significant improvement in correlating thermodynamic properties of pure fluids and mixtures.^{23,24}

In the PHSC equation of state, parameter b represents the excluded volume on a segment basis. For

diblock copolymers consisting of two types of segments A and B, parameter b is given by

$$b_{\alpha} = b_{\alpha\alpha} = {}^2/3\pi\sigma_{\alpha}^3 \quad (\alpha = A, B) \quad (20)$$

$$b_{AB} = b_{BA} = {}^1/8(b_A^{1/3} + b_B^{1/3})^3 \quad (21)$$

In terms of parameter b , the reference Helmholtz energy is given by

$$\left(\frac{A}{Nk_B T}\right)_{\text{ref}} = \rho(r_A^2 b_A Z_{AA} + 2r_A r_B b_{AB} Z_{AB} + r_B^2 b_B Z_{BB}) - [r_{AA} Q_{AA} + r_{AB} Q_{AB} + r_{BB} Q_{BB}] \quad (22)$$

where the first term in the right-hand side of eq 22 represents the Helmholtz energy of hard-sphere mixtures prior to bonding to form a hard-sphere chain and the second term represents chain connectivity with $r_{\alpha\beta}$ ($\alpha, \beta = A, B$) given by eq 2. In eq 22, functions Z and Q are given by

$$Z_{\alpha\beta} = \frac{1}{\eta} I_1 + {}^3/2 \frac{\xi_{\alpha\beta}^2}{\eta^2} I_2 + {}^1/2 \frac{\xi_{\alpha\beta}^2}{\eta^3} I_3 \quad (\alpha, \beta = A, B) \quad (23)$$

$$Q_{\alpha\beta} = -\ln(1 - \eta) + {}^3/2 \frac{\xi_{\alpha\beta}}{1 - \eta} + {}^1/4 \frac{\xi_{\alpha\beta}^2}{(1 - \eta)^2} \quad (24)$$

where

$$\xi_{\alpha\beta} = \frac{\rho}{4} \left(\frac{b_{\alpha} b_{\beta}}{b_{\alpha\beta}} \right)^{1/3} (r_A b_A^{2/3} + r_B b_B^{2/3}) \quad (25)$$

$$I_1 = -\ln(1 - \eta) \quad (26)$$

$$I_n = -I_{n-1} + \frac{1}{n-1} \frac{\eta^{n-1}}{(1 - \eta)^{n-1}} \quad (n > 2) \quad (27)$$

The perturbation term is based on the second-order perturbation theory for the square-well fluid of variable well width presented in ref 25. The square-well potential is defined by

$$u(R) = \begin{cases} \infty & R < \sigma \\ -\epsilon & \sigma \leq R < \lambda\sigma \\ 0 & R \geq \lambda\sigma \end{cases} \quad (28)$$

where $u(R)$ is the pair potential, R is the intersegmental center-to-center distance between nonbonded segments, σ is the hard-sphere diameter, ϵ is the depth of the well, and λ is the reduced well width. Although ref 25 considers only homogeneous molecules consisting of one kind of segment (e.g., homopolymers), we also apply the perturbation terms given in ref 25 to copolymers consisting of two kinds of segments by replacing parameters for homogeneous molecules by those for copolymers averaged over the copolymer composition.

The perturbation term is given by

$$\left(\frac{A}{Nk_B T}\right)_{\text{pert}} = \left(\frac{A_1}{Nk_B T}\right)_{\text{pert}} + \left(\frac{A_2}{Nk_B T}\right)_{\text{pert}} \quad (29)$$

where A_1 and A_2 are the first- and second-order pertur-

Table 1. Coefficients c_k for Function Ψ with $\lambda = 1.455$

c_1	0.6934288007E+00
c_2	0.1031329977E+01
c_3	0.3231430915E+00
c_4	-0.7601028313E+00
c_5	-0.1898718617E+01
c_6	-0.1129836508E+01
c_7	-0.5829453430E+00
c_8	-0.4161049123E+01
c_9	-0.8040279885E+01
c_{10}	0.2470320458E+02

bation terms, respectively, for the Helmholtz energy given by²⁵

$$\left(\frac{A_1}{Nk_B T}\right)_{\text{pert}} = -\frac{\langle r^2 b \epsilon \rangle}{k_B T} \rho \Psi \quad (30)$$

$$\left(\frac{A_2}{Nk_B T}\right)_{\text{pert}} = -{}^1/2 \frac{\langle r^2 b \epsilon^2 \rangle}{(k_B T)^2} \rho \frac{(1 - \eta)^4}{(1 + 4\eta + 4\eta^2)} \left(\Psi + \eta \frac{\partial \Psi}{\partial \eta} \right) \quad (31)$$

where

$$\langle r^2 b \epsilon^m \rangle = r_A^2 b_A \epsilon_A^m + 2r_A r_B b_{AB} \epsilon_{AB}^m + r_B^2 b_B \epsilon_B^m \quad (m = 1, 2) \quad (32)$$

$$\epsilon_{AB} = (1 - \kappa_{AB}) \sqrt{\epsilon_A \epsilon_B} \quad (33)$$

where κ_{AB} is an adjustable binary parameter. Equation 33 is used only to introduce an adjustable binary parameter. As shown later, the theoretical phase diagrams of polymer blends and those of diblock copolymer melts are very sensitive to κ_{AB} . The geometric mean of ϵ_A and ϵ_B cannot be used to predict ϵ_{AB} . The interaction parameter between segments A and B must be obtained by correlating thermodynamic properties of systems containing both segments A and B.

In eqs 30 and 31, Ψ is a function of η and λ resulting from integration of the radial distribution function for hard spheres over the width of the well. In this work, the reduced well width λ is 1.455 for all fluids; $\lambda = 1.455$ is the optimum value for methane with $r = 1$.²⁵ Function Ψ is obtained by fitting²⁵ the analytic equation for Ψ in the range of $1 < \lambda \leq 2$ given by Chang and Sandler²⁹ to a polynomial function of η :

$$\Psi(\eta) = 3 \sum_{k=1}^{10} c_k \eta^{k-1} \quad (34)$$

For $\lambda = 1.455$, Table 1 gives numerical coefficients c_k . As shown in ref 25, the optimum reduced well width (here $\lambda = 1.455$) can be assigned to each segment combined with appropriate mixing rules for the perturbation term.

As discussed in ref 25, the quality of fits is sensitive to λ when the equation-of-state parameters of a normal fluid are obtained from the saturated vapor pressure and liquid density of the saturated liquid. The PHSC equation of state, however, provides excellent correlations of homopolymer pressure–volume–temperature (pVT) data for several values of λ including $\lambda = 1.455$. It is not possible to obtain the optimum reduced well width based solely on the quality of fits of homopolymer pVT data. Therefore, we use the PHSC equation of state with $\lambda = 1.455$ that correlates very well both the

thermodynamic properties of saturated liquids and pVT data of homopolymer melts.

To calculate the interaction matrix for the RPA, the Helmholtz energy density is required. From eq 18, the Helmholtz energy density is given by

$$\frac{\Delta A}{Vk_B T} = \frac{\eta}{rv} \ln \left(\frac{\eta k_B T}{rv} \right) + \left(\frac{A}{Vk_B T} \right)_{\text{ref}} + \left(\frac{A}{Vk_B T} \right)_{\text{pert}} \quad (35)$$

where r is the number of segments per molecule, v is the average segment volume given by eq 13, and η is the packing fraction given by eq 4. The leading term in the right-hand side of eq 35 resembles the translational entropy of polymers in the Flory–Huggins theory.^{13,16,18} Therefore, the sum of the reference and perturbation terms in eq 35 are identified as the nonideal Helmholtz energy density for the PHSC theory. This nonideal Helmholtz energy is used to obtain the interaction matrix for the RPA.

The next step is to express the nonideal Helmholtz energy density in terms of η_A and η_B , the packing fractions of segments A and B. Using eqs 22, 30, and 31, the nonideal Helmholtz energy density is given by

$$\begin{aligned} \left(\frac{\Delta A}{Vk_B T} \right)_{\text{ref+pert}} &= \frac{16}{b_A b_B} (\eta_A^2 b_B Z_{AA} + 2\eta_A \eta_B b_{AB} Z_{AB} + \\ &\eta_B^2 b_A Z_{BB}) - 4 \left[\frac{\eta_A}{b_A} Q_{AA} + \frac{\eta_B}{b_B} Q_{BB} \right] - \frac{\eta}{rv} [-Q_{AA} + Q_{AB} - \\ &Q_{BB}] + \left(\frac{A_1}{Vk_B T} \right)_{\text{pert}} + \left(\frac{A_2}{Vk_B T} \right)_{\text{pert}} \quad (36) \end{aligned}$$

where the subscript ref+pert denotes the nonideal Helmholtz energy density consisting of the reference and perturbation terms for the PHSC theory and

$$\left(\frac{A_1}{Vk_B T} \right)_{\text{pert}} = -\frac{16}{b_A b_B} \left[\eta_A^2 b_B \left(\frac{\epsilon_A}{k_B T} \right) + 2\eta_A \eta_B b_{AB} \left(\frac{\epsilon_{AB}}{k_B T} \right) + \eta_B^2 b_A \left(\frac{\epsilon_B}{k_B T} \right) \right] \Psi \quad (37)$$

$$\begin{aligned} \left(\frac{A_2}{Vk_B T} \right)_{\text{pert}} &= -\frac{8}{b_A b_B} \left[\eta_A^2 b_B \left(\frac{\epsilon_A}{k_B T} \right)^2 + 2\eta_A \eta_B b_{AB} \left(\frac{\epsilon_{AB}}{k_B T} \right)^2 + \right. \\ &\left. \eta_B^2 b_A \left(\frac{\epsilon_B}{k_B T} \right)^2 \right] \frac{(1-\eta)^4}{(1+4\eta+4\eta^2)} \left(\Psi + \eta \frac{\partial \Psi}{\partial \eta} \right) \quad (38) \end{aligned}$$

In terms of η_A and η_B , $\xi_{\alpha\beta}$ in functions Q and Z are given by

$$\begin{aligned} \xi_{AA} &= \eta_A + \eta_B \left(\frac{b_A}{b_B} \right)^{1/3}, & \xi_{BB} &= \eta_A \left(\frac{b_B}{b_A} \right)^{1/3} + \eta_B, \\ \xi_{AB} &= \eta_A \left(\frac{b_B}{b_{AB}} \right)^{1/3} + \eta_B \left(\frac{b_A}{b_{AB}} \right)^{1/3} \quad (39) \end{aligned}$$

Finally, the elements of the interaction matrix are given by

$$W_{ij} = \left[\frac{\partial^2 \left(\frac{\Delta A}{Vk_B T} \right)_{\text{ref+pert}}}{\partial \eta_j \partial \eta_i} \right]_{V,T,\eta_k} \quad (i, j = 1, 2) \quad (40)$$

where subscripts 1 and 2 denote segments A and B,

Table 2. Equation-of-State Parameters for Homopolymers with $\lambda = 1.445$

polymer	r/M (mol/g)	σ (Å)	ϵ/k_B (K)	% rms ^a deviation	
				ρ_{liq}	ref ^b
poly(<i>cis</i> -1,4-butadiene)	0.03382	3.631	329.2	0.07	30 (63) ^c
polystyrene	0.02123	4.059	409.9	0.09	31 (69)
poly(α -methylstyrene)	0.02188	3.965	414.5	0.15	32 (86)
poly(<i>n</i> -butyl methacrylate)	0.02942	3.595	311.5	0.24	33 (168)
poly(vinyl methyl ether)	0.03053	3.571	299.9	0.05	34 (66)

^a Root-mean-square relative deviations. ^b Reference. ^c Numbers in parentheses indicate numbers of data points used in the correlations.

respectively. Subscript η_k denotes that the derivative with respect to η_i is taken while the other $\eta_{k \neq i}$ is held constant.

III. Results and Discussion

We first note common shortcomings of molecular thermodynamic models, including the PHSC equation of state, that become apparent when models are applied to fit experimental data for real systems. Although theories for polymeric fluids use molecular parameters that are independent of temperature and polymer molecular weight, the theoretical phase diagrams of mixtures do not always show quantitative agreement with experiment over the entire range of polymer molecular weight and temperature. In addition, it is a challenging task to correlate both UCST and LCST behaviors of polymer solutions and blends using only one adjustable binary parameter. To correlate quantitatively the phase diagrams of mixtures, it is often necessary to introduce a temperature dependence in the binary adjustable parameter or to use several binary parameters.

In equation-of-state theories for polymer blends, the theoretical phase diagrams are also sensitive to pure-component parameters. To achieve quantitative correlations of the phase diagrams of mixtures by equation-of-state theories, the pure-component parameters of one polymer may be slightly adjusted from those that give the optimum correlations of pure-component data.

1. Computation Procedure. To apply the PHSC equation of state to real diblock copolymer melts, theory requires three equation-of-state parameters for each of the parent homopolymers: segment diameter σ , well depth ϵ , and r/M where r is the number of segments per molecule and M is the molecular weight of the polymer. To compute r for a given polymer, we use the weight-average molecular weight of the polymer M_w . The PHSC equation of state can then describe thermodynamic properties of a homopolymer melt.

For homopolymers, the equation-of-state parameters are regressed from pure-component pressure–volume–temperature (pVT) data^{30–34} in the liquid state. Table 2 gives the PHSC equation-of-state parameters with $\lambda = 1.455$ for common polymers studied in this work. For each homopolymer, these parameters were regressed from the pVT data over the entire liquid range reported in the literature. Experimental pVT data are usually collected to about 2000 bar. However, pure-component pVT data for poly(vinyl methyl ether) (PVME) are not tabulated in the literature. Therefore, pVT data for PVME were simulated in the range 100–200 °C and 1–500 bar by the Simha–Somcynsky equation of state³⁴

using the parameters given by Rodgers.³⁴ Except for poly(α -methylstyrene), the equation-of-state parameters given in Table 2 are those that give the optimum correlations of pVT data.

In the present theory, we use the optimum set of equation-of-state parameters regressed from experimental pVT data because there is no physical basis for representing the repeat unit of the homopolymer by a single sphere. It is possible to establish correlations between the chemical structure of the homopolymer and the equation-of-state parameters that give the optimum correlations of homopolymer pVT data.³⁵

For poly(α -methylstyrene), we use another set of equation-of-state parameters because theory with these parameters correlates better the dependence of coexistence curves on the molecular weight of the polymer in the blend polystyrene/poly(α -methylstyrene). The equation-of-state parameters for poly(α -methylstyrene) were obtained by first presetting σ to a reasonable value and then regressing for ϵ and r/M . For all homopolymers including poly(α -methylstyrene), the PHSC equation of state provides excellent correlations of pure-component pVT data.

The PHSC equation of state also requires adjustable binary parameter κ_{AB} (in eq 33) that reflects the strength of attractive interaction between a pair of unlike segments A and B. In this work, parameter κ_{AB} is obtained from the coexistence curve for the binary blend containing parent homopolymers. Details of the PHSC equation of state for homopolymer blends are given in ref 25.

With κ_{AB} obtained in this manner, the function $F(q)$ defined by eq 17 is used to predict the stability limit for a disordered diblock copolymer melt. The stability limit is defined as the extreme temperature when the temperature that satisfies $F(q) = 0$ is plotted against q . This extreme temperature is the order-to-disorder transition temperature of a diblock copolymer melt. Equation 17 expresses $F(q)$ in terms of the second-order vertex functions defined by eq 16.

Similar to the incompressible model of Leibler,¹⁵ in the plot of temperature that satisfies $F(q) = 0$, our compressible model also gives the extreme temperature at $x^* \cong 4.0$ that is nearly independent of the polymer molecular weight and copolymer composition. (x^* is related to the wave number q^* by eq 15.) Therefore, unless otherwise specified, we report the temperature that satisfies $F(q^*(x^*)) = 0$ at $x^* = 4.0$ as the order-to-disorder transition temperature of a diblock copolymer melt.

In this work, the packing fraction of a disordered system is used as the packing fraction in the second-order vertex functions. The packing fraction of a disordered system is calculated through eq 19 using eqs 22 and 29 as the reference and perturbation terms, respectively, for the Helmholtz energy. Unless otherwise specified, all calculations are made at zero pressure, an excellent approximation for diblock copolymer melts and homopolymer blends near atmospheric pressure.

2. Poly(styrene-*block*- α -methylstyrene). We first apply the model to poly(styrene-*block*- α -methylstyrene) (PS-PMS) diblock copolymer melts. Because the chemical structure of polystyrene (PS) is similar to that of poly(α -methylstyrene) (PMS), the homopolymer blend PS/PMS is one of few nearly compatible polymer blends that exhibit UCST behavior in the temperature range

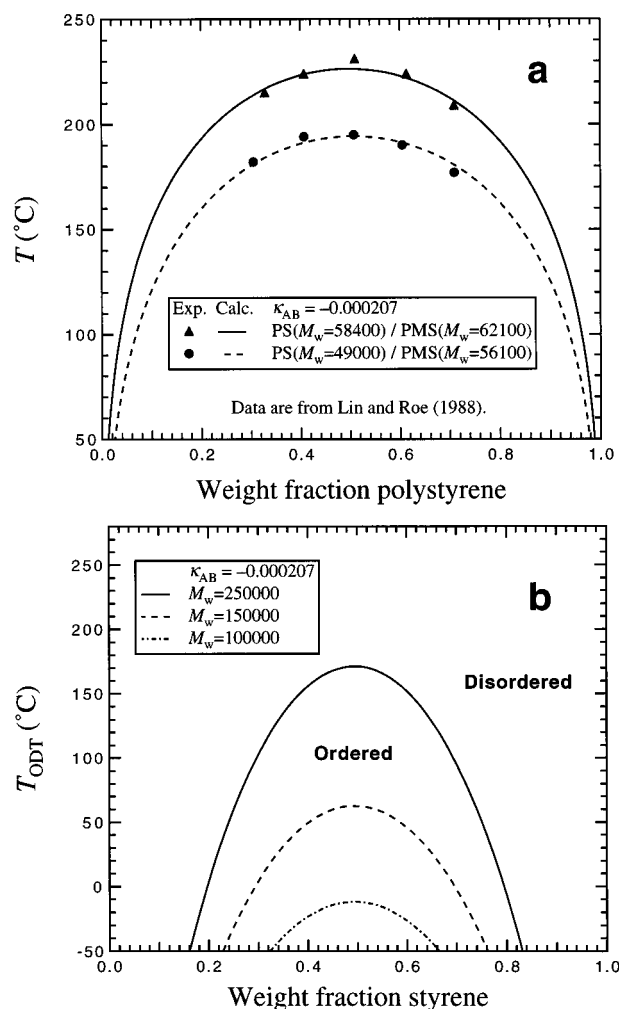


Figure 2. (a) Comparison of theoretical coexistence curves with experiment for the system polystyrene/poly(α -methylstyrene)³⁶ (PS/PMS, $\kappa_{AB} = -0.000207$). (b) Predicted T_{ODT} for PS-PMS diblock copolymer melts as functions of polymer molecular weight in g/mol and copolymer composition. For the molecular weights shown in part b, experiments show that the PS-PMS diblock copolymers have T_{ODT} below 170 °C (i.e., below the glass-transition temperature of PMS).^{37,38}

accessible by standard experiments. The miscible blend of PS with PMS, however, does not exhibit LCST behavior at elevated temperatures, probably because the disparity in compressibility between PS and PMS is not strong enough to induce phase separation at elevated temperatures. All experimental data used here are those obtained with nearly monodispersed polymers having polydispersity indices of less than 1.09.

Binary parameter κ_{AB} between styrene and α -methylstyrene segments is obtained from coexistence curves for the homopolymer blend PS/PMS reported by Lin and Roe.³⁶ Figure 2a compares the theoretical coexistence curves with experiment for the system PS($M_w = 49000$)/PMS($M_w = 56100$) and system PS($M_w = 58400$)/PMS($M_w = 62100$). The PHSC equation of state for binary homopolymer blends is given in ref 24. Theory and experiment show good agreement using $\kappa_{AB} = -0.000207$. Consistent with experiment, theory predicts only UCST behavior in the system shown in Figure 2a.

Using binary parameter $\kappa_{AB} = -0.000207$, we can predict the order-to-disorder transition temperature T_{ODT} for PS-PMS diblock copolymer melts that show UCOT behavior. Although precise measurements of

T_{ODT} are not reported for PS–PMS diblock copolymers, there are several PS–PMS diblock copolymers having different molecular weights and copolymer compositions that are known to be either in the disordered or in the ordered state at a given temperature.³⁶

Figure 2b shows the predicted T_{ODT} for PS–PMS diblock copolymer melts as functions of polymer molecular weight in g/mol and copolymer composition. The shape of curves in this figure resembles the coexistence curves of parent homopolymer blends shown in Figure 2a. However, the ordered region in Figure 2b is narrow compared to the two-phase region in Figure 2a. Consistent with the incompressible model of Leibler,¹⁵ for a symmetric diblock copolymer, the highest molecular weight of diblock copolymer that is disordered at T^* is about 5 times larger than the molecular weight of parent homopolymers whose mixtures give a critical temperature T^* .

Using differential scanning calorimetry and rheological measurements, Kim and Han report that the order-to-disorder transition temperatures of PS($M_w = 120000$)–PMS($M_w = 135000$) and PS($M_w = 130000$)–PMS($M_w = 50000$) diblock copolymer melts should lie below 170 °C (i.e., below the glass transition temperature of PMS).^{37,38} Our model predicts T_{ODT} at 175 and 14 °C for PS($M_w = 120000$)–PMS($M_w = 135000$) and PS($M_w = 130000$)–PMS($M_w = 50000$), respectively.

The present model slightly overestimates T_{ODT} for PS–PMS diblock copolymer melts. Kim and Han³⁷ mention that when the RPA is combined with incompressible Flory–Huggins theory, the prediction also overestimates T_{ODT} for PS–PMS diblock copolymer melts when the binary parameter is obtained from the phase diagrams shown in Figure 2a. As discussed by Fredrickson and Helfand,³⁹ a possible explanation for this behavior is the fluctuation effect that is not considered in the present model. For a given binary parameter between copolymer segments, the theory by Fredrickson and Helfand³⁹ (that includes the fluctuation effect) predicts T_{ODT} associated with UCOT at a temperature lower than the T_{ODT} predicted by the theory that neglects the fluctuation effect. The fluctuation effect is negligible only in the limit of infinite molecular weight of diblock copolymers.³⁹ Because the RPA calculation is a total prediction, agreement of theoretical prediction with experiment is encouraging.

Similar to other equation-of-state theories, our theoretical phase diagrams of polymer blends are also sensitive to binary parameter κ_{AB} . For the system PS($M_w = 58400$)/PMS($M_w = 62100$) shown in Figure 2a, the theoretical UCST with $\kappa_{AB} = -0.000107$ is about 140 °C higher than that with $\kappa_{AB} = -0.000207$. Similarly, for the diblock copolymer PS($M_w = 120000$)–PMS($M_w = 135000$) shown in Figure 2b, the theoretical UCOT with $\kappa_{AB} = -0.000107$ is about 120 °C higher than that with $\kappa_{AB} = -0.000207$.

3. Poly(styrene-*block*-butadiene). The order-to-disorder transition temperature associated with UCOT is also reported for a poly(styrene-*block*-butadiene) (PS–PBD) diblock copolymer melt by Zin and Roe.^{40,41} For PS–PBD diblock copolymer melts, the binary parameter κ_{AB} between styrene and butadiene segments is obtained from the cloud-point curves for the homopolymer blend PS/PBD reported by Roe and Zin.⁴² Figure 3a compares the theoretical coexistence curves with experiment for the system PS($M_w = 3500$)/PBD($M_w = 2660$) and system PS($M_w = 2400$)/PBD($M_w = 2660$). Although

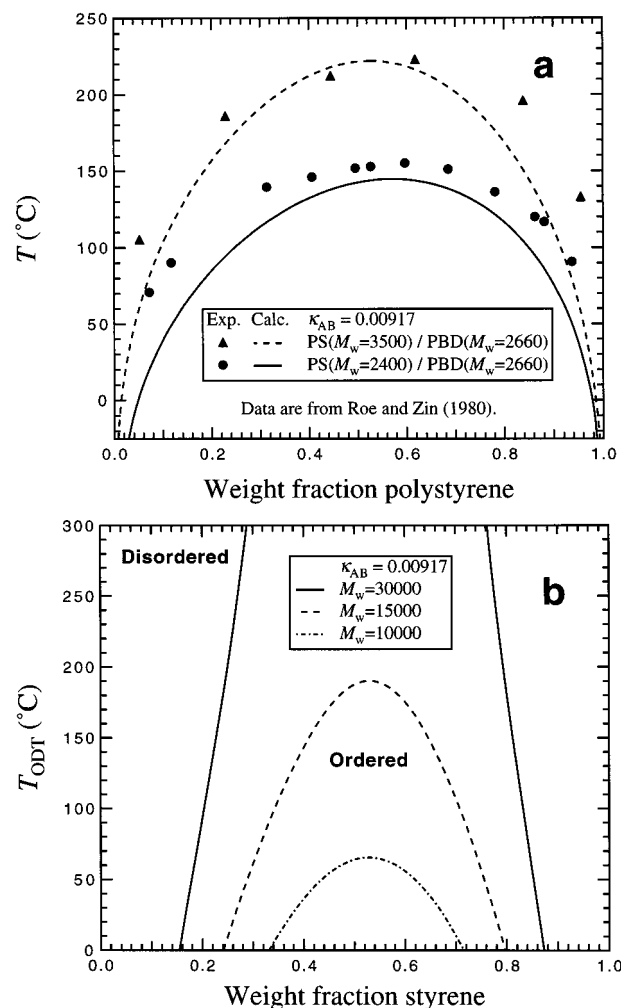


Figure 3. (a) Comparison of theoretical coexistence curves with experiment for the system polystyrene/polybutadiene⁴² (PS/PBD, $\kappa_{AB} = 0.00917$). (b) Predicted T_{ODT} for PS–PBD diblock copolymer melts as functions of polymer molecular weight in g/mol and copolymer composition. For the PS($M_w = 7600$)–PBD($M_w = 20400$) diblock copolymer, the predicted T_{ODT} associated with UCOT is about 70 °C higher than the measurement by Zin and Roe.^{40,41}

theory quantitatively represents the dependence of UCST on the molecular weight of PS, the theoretical coexistence curves are narrow compared to experiment.

Using $\kappa_{AB} = 0.00917$ obtained from part a of Figure 3, part b of Figure 3 shows the predicted T_{ODT} for PS–PBD diblock copolymer melts as functions of polymer molecular weight in g/mol and copolymer composition. Similar to the systems containing PS and PMS shown in Figure 2, the ordered region of diblock copolymer melts in part b of Figure 3 is narrow compared to the two-phase region of parent homopolymer blends in part a of Figure 3. For PS–PBD diblock copolymer melts, T_{ODT} is sensitive to both polymer molecular weight and copolymer composition.

For the PS($M_w = 7600$)–PBD($M_w = 20400$) diblock copolymer melt studied by Roe and Zin,^{40,41} the theoretical T_{ODT} is 215 °C that is about 70 °C higher than the measured T_{ODT} . For this diblock copolymer, Han et al.⁴³ also report that the RPA combined with the incompressible Flory–Huggins theory predicts T_{ODT} at 221 °C. Similarly, the analysis based on the Hong–Noolandi theory by Baek et al.⁴⁴ predicts T_{ODT} at about 215 °C for the same diblock copolymer.

In addition to the fluctuation effect,³⁹ for PS–PBD diblock copolymer melts, the discrepancy between theoretical prediction and measured T_{ODT} may be caused by the uncertainty in binary parameter κ_{AB} because κ_{AB} between styrene and butadiene segments is obtained from the mixtures of oligomers shown in Figure 3a. Furthermore, this discrepancy may also be due to the difference between the microstructure of the PBD homopolymer used in ref 42 and that of the PBD block in the PS–PBD diblock copolymer studied in refs 40 and 41. All polymers considered in Figure 3a,b are essentially monodispersed having polydispersity indices less than 1.13.

For systems such as PS–PMS and PS–PBD diblock copolymer melts that show only UCOT behavior, predicted order-to-disorder transition temperatures by the present model may be close to those predicted by the RPA combined with the incompressible Flory–Huggins theory.^{15,18,37}

4. Poly(styrene-*block-n*-butyl methacrylate).

Next, we consider the poly(styrene-*block-n*-butyl methacrylate) diblock copolymer melt that has recently been found to exhibit both an UCOT and a LCOT by Russell et al.^{10–12} All experimental data in this section use deuterated polystyrene (PSD); the diblock copolymer consisting of PSD and poly(*n*-butyl methacrylate) (PBMA) is denoted as PSD–PBMA. Phase equilibrium calculations, however, are performed using the equation-of-state parameters for normal polystyrene. For theoretical calculations, the poly(styrene-*block-n*-butyl methacrylate) diblock copolymer is denoted as PS–PBMA.

Shortly after the discovery of both UCOT and LCOT behaviors in PSD–PBMA diblock copolymer melts, Hammouda et al.¹¹ used small-angle neutron scattering to show that the parent homopolymer blend PSD/PBMA exhibits both an UCST and a LCST in a temperature–composition diagram. These experiments on the system containing PSD and PBMA indicate that the phase behavior of a diblock copolymer melt that exhibits both an UCOT and a LCOT also follows closely the phase behavior of the binary blend containing parent homopolymers.

Using the PHSC equation of state, our main objective here is to establish a quantitative relation between the phase behavior of PS–PBMA diblock copolymer melts and that of binary homopolymer blends containing PS and PBMA. To perform quantitative analysis, it is necessary to use a unique set of binary and equation-of-state parameters for diblock copolymer melts as well as for parent homopolymer blends.

Consistent with experiment, the PHSC equation of state predicts both an UCST and a LCST in a temperature–composition diagram for homopolymer blends containing PS and PBMA. Theory also predicts UCOT behavior as well as LCOT behavior in PS–PBMA diblock copolymer melts. Using $\kappa_{AB} = 0.00782$, parts a and b of Figure 4 show, respectively, the theoretical coexistence curves for the blend PS/PBMA and the theoretical T_{ODT} for PS–PBMA diblock copolymer melts as functions of polymer molecular weight and copolymer composition. Binary parameter κ_{AB} was adjusted such that theory roughly agrees with experiment for both homopolymer blends⁹ and diblock copolymer melts^{10,12} for the molecular weights shown in Figure 4.

The numbers in Figure 4 are the molecular weights of homopolymers and the molecular weights of blocks comprising diblock copolymers in g/mol. In part b of

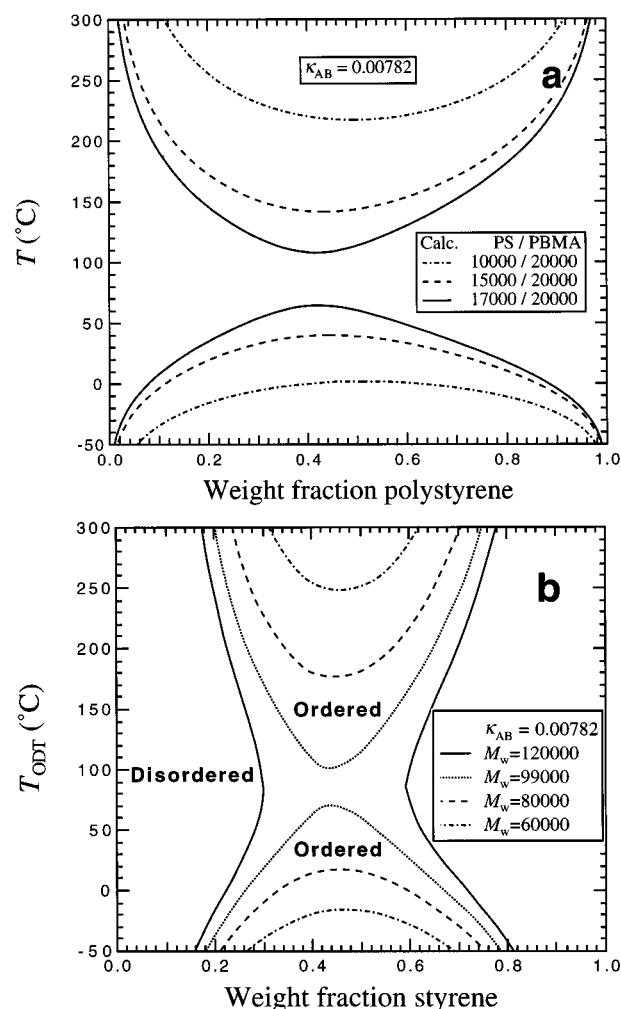


Figure 4. Theoretical phase diagrams for systems containing polystyrene (PS) and poly(*n*-butyl methacrylate) (PBMA) with $\kappa_{AB} = 0.00782$. (a) Coexistence curves for the homopolymer blend PS/PBMA. (b) T_{ODT} for PS–PBMA diblock copolymer melts as functions of polymer molecular weight in g/mol and copolymer composition. For the 47000-*block*-52000 diblock copolymer, theoretical UCOT and LCOT are about 20 °C lower than those determined by rheological measurements.¹² The numbers in these figures denote the molecular weights of parent homopolymers and those of blocks comprising diblock copolymers in g/mol.

Figure 4, an hourglass-type phase diagram is obtained as the molecular weight of PS–PBMA diblock copolymer rises. In an hourglass-type phase diagram, there is no temperature range where the diblock copolymer is disordered over the entire copolymer composition.

For the homopolymer blend PS/PBMA shown in Figure 4a, precise comparison of theory with experiment by Hammouda et al.¹¹ is difficult because the exact locations of cloud-point temperatures are not reported. In addition, the polymers used by Hammouda et al.¹¹ are polydisperse with polydispersity indices of about 2.0. Nevertheless, theoretical UCSTs and LCSTs are at least in semiquantitative agreement with experiment for the molecular weights shown in Figure 4a.¹¹

The PSD–PBMA diblock copolymers studied by Russell et al.^{10,12} are nearly monodisperse with polydispersity indices of less than 1.04. For the 47000-*block*-52000 PS–PBMA diblock copolymer, theoretical UCOT and LCOT are 70 and 101 °C, respectively, that are about 20 °C lower than those determined by rheological measurements.¹² For the 34500-*block*-33500 PS–

PBMA diblock copolymer, theoretical UCOT and LCOT are -4 and 219 °C, respectively. The rheological measurements¹² on the sample 34500-*block*-33500 indicate that this copolymer is in the disordered state from 100 to 275 °C. Therefore, theory with $\kappa_{AB} = 0.00782$ may underestimate LCOT and UCOT for PS–PBMA diblock copolymer melts.

Overall agreement of theory with experiment is encouraging for the system containing PS and PBMA. Using the same set of binary and equation-of-state parameters, the PHSC equation of state shows semi-quantitative agreement with experiment for the phase behavior of diblock copolymer melts as well as that for parent homopolymer blends. We conclude that within the prediction by the PHSC equation of state combined with the RPA, the LCOT and UCOT behavior for PS–PBMA diblock copolymer melts follows closely the LCST and UCST behavior for PS/PBMA homopolymer blends.

For PS–PBMA diblock copolymer melts that exhibit both UCOT and LCOT behaviors, the RPA combined with the compressible lattice-cluster theory¹⁹ and that combined with the lattice-fluid equation of state²⁸ (i.e., a compressible Flory–Huggins theory) may also predict the results similar to those obtained with the PHSC equation of state. Although the PHSC equation of state correlates pVT data of homopolymer melts slightly better than the lattice-fluid equation of state and the compressible lattice-cluster theory,^{25,35,45} the latter theories are also capable of predicting both UCST and LCST behaviors in homopolymer blends. However, to provide a fair comparison of the PHSC equation of state with the above-mentioned compressible lattice theories, it would be necessary to perform consistent fitting procedures to obtain both the pure-component and binary parameters.

5. Poly(styrene-*block*-vinyl methyl ether). As an example of phase separation at elevated temperatures, we also consider systems containing polystyrene (PS) and poly(vinyl methyl ether) (PVME). The binary blend of PS and PVME has been extensively studied because this blend shows LCST behavior in the temperature range readily accessible by a scattering experiment. Recently, Hashimoto et al.²⁰ performed a small-angle neutron-scattering analysis on a disordered diblock copolymer melt consisting of deuterated polystyrene (PSD) and PVME. (The diblock copolymer consisting of PSD and PVME is denoted as PSD–PVME diblock copolymer.) Between 34 and 206 °C, Hashimoto et al. did not detect the disorder-to-order transition by heating the disordered PSD($M_w = 9000$)–PVME($M_w = 14000$) diblock copolymer melt. However, as indicated by the increased scattered intensity with temperature, LCOT behavior may exist for this PSD–PVME diblock copolymer.²⁰

For PS and PVME, binary parameter κ_{AB} is obtained from the coexistence curves of the homopolymer blend PS/PVME reported by Walsh et al.⁴⁶ Figure 5a compares the theoretical coexistence curves with experiment for the system PS($M_w = 233000$)/PVME($M_w = 95000$) and system PS($M_w = 106000$)/PVME($M_w = 45000$). Consistent with experiment, theory predicts LCST behavior in the blend PS/PVME. In addition, theory correctly predicts the critical mixture composition that is rich in PVME. However, theoretical coexistence curves are narrow compared to experiment.

Using $\kappa_{AB} = 0.00785$ obtained from the parent homopolymer blend PS/PVME, part b of Figure 5 shows the predicted T_{ODT} for PS–PVME diblock copolymer

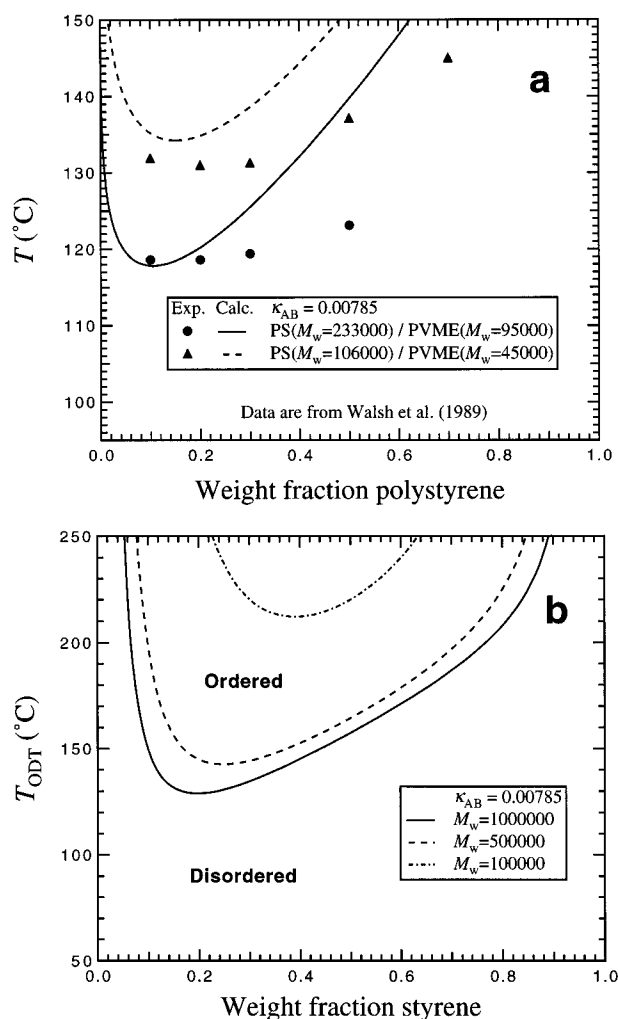


Figure 5. (a) Comparison of theoretical coexistence curves with experiment for the system polystyrene/poly(vinyl methyl ether)⁴⁶ (PS/PVME, $\kappa_{AB} = 0.00785$). (b) Predicted T_{ODT} for PS–PVME diblock copolymer melts as functions of polymer molecular weight in g/mol and copolymer composition. Experiment shows that the PSD($M_w = 9000$)–PVME($M_w = 14000$) diblock copolymer is disordered between 34 and 206 °C.²⁰

melts as functions of polymer molecular weight in g/mol and copolymer composition. T_{ODT} is calculated using equation-of-state parameters for normal polystyrene. For theoretical calculations, the poly(styrene-*block*-vinyl methyl ether) diblock copolymer is denoted as PS–PVME. Similar to the blend PS/PVME, our model predicts a highly asymmetric phase diagram in PS–PVME diblock copolymer melts. Consistent with the experiment of Hashimoto et al.,²⁰ our model predicts that the PS($M_w = 9000$)–PVME($M_w = 14000$) diblock copolymer is disordered between 34 and 206 °C.

6. Effect of Pressure. Finally, we consider the effect of pressure on the phase behavior of diblock copolymer melts and that of the binary blends containing parent homopolymers studied in this work.

For diblock copolymer melts that exhibit UCOT behavior, the pressure dependence of T_{ODT} was recently measured for styrene–isoprene (SI),⁴⁷ (ethylene–propylene)–ethylene (PEP–PEE),⁴⁸ and (ethylene–propylene)–dimethylsiloxane (PEP–PDMS)⁴⁹ diblock copolymers. The measured T_{ODT} shows complicated dependence on the pressure. While T_{ODT} for SI diblock copolymers rises with increasing pressure at a rate of about +20 °C/kbar over the range 0–0.6 kbar,⁴⁷ T_{ODT}

for PEP-PEE diblock copolymers decreases with increasing pressure at a rate of about $-20\text{ }^{\circ}\text{C/kbar}$ for pressures up to 1 kbar.⁴⁸ On the other hand, T_{ODT} for PEP-PDMS diblock copolymers first decreases and then rises with increasing pressure over the range 0–1.5 kbar.⁴⁹

A theoretical study by Dudowicz and Freed^{19,50} investigated the effect of pressure on the phase behavior of diblock copolymer melts and that of binary blends containing parent homopolymers. Using the compressible lattice-cluster theory, Dudowicz and Freed¹⁹ presented a semiquantitative analysis of systems containing PS and poly(vinyl methyl ether) (PVME). Both experiment and theory show that the homopolymer blend of PS and PVME exhibits LCST behavior. The theory by Dudowicz and Freed¹⁹ predicts that a disordered PS-PVME diblock copolymer melt exhibits disorder-to-order transition upon heating. Recently, Dudowicz and Freed⁵⁰ also presented a more rigorous analysis of the homopolymer blend of PS and PVME by the compressible lattice-cluster theory.

We now discuss the predicted pressure dependence of T_{ODT} by the PHSC equation of state. In the plot of temperature that satisfies $F(q) = 0$, the extreme temperature (i.e., T_{ODT}) occurs at x^* that is nearly independent of pressure. (x^* is related to the wavenumber q^* by eq 15.) Therefore, for each system, T_{ODT} is computed as a function of pressure from the condition $F(q^*) = 0$ using q^* at zero pressure. We assume that binary parameter κ_{AB} is independent of pressure.

For systems containing PS and PMS discussed in Figure 2, part a of Figure 6 shows the predicted pressure dependence of critical solution temperature (T_c) for a PS/PMS blend and that of T_{ODT} for a PS-PMS diblock copolymer melt. For the PS($M_w = 120000$)-PMS($M_w = 135000$) diblock copolymer, the maximum temperature occurs at $x^* = 3.8$ in the plot of temperature that satisfies $F(q) = 0$. These systems show UCOT behavior in the diblock copolymer melt and UCST behavior in the binary blend of parent homopolymers. As the pressure rises, the predicted T_c and T_{ODT} first decrease and then become almost independent of pressure.

For systems containing PS and PBD discussed in Figure 3, part b of Figure 6 shows the pressure dependence of predicted T_c for a PS/PBD blend and that of T_{ODT} for a PS-PBD diblock copolymer melt. For the PS($M_w = 7600$)-PBD($M_w = 20400$) diblock copolymer, the maximum temperature occurs at $x^* = 4.2$ in the plot of temperature that satisfies $F(q) = 0$. These systems also show UCST and UCOT behavior. For the PS-PBD diblock copolymer shown in Figure 6b, the predicted T_{ODT} rises with increasing pressure. Recent experiment by Hadjuk et al.⁴⁷ shows that for styrene-isoprene diblock copolymers that exhibit UCOT behavior, the measured T_{ODT} also rises with increasing pressure at a rate of about $+20\text{ }^{\circ}\text{C/kbar}$ over the range 0–0.6 kbar. Because the structure of isoprene is similar to that of butadiene, for styrene-diene diblock copolymers, there may be a general trend that T_{ODT} associated with UCOT behavior rises with increasing pressure.

For systems containing PS and PBMA shown in Figure 4, Figure 7a shows the predicted pressure dependence of T_c for a PS/PBMA blend (exhibiting both UCST and LCST behaviors) and that of T_{ODT} for a PS-PBMA diblock copolymer melt (exhibiting both UCOT and LCOT behaviors). For the PS($M_w = 47000$)-PBMA($M_w = 52000$) diblock copolymer, the maximum temperature occurs at $x^* = 3.8$ in the plot of tempera-

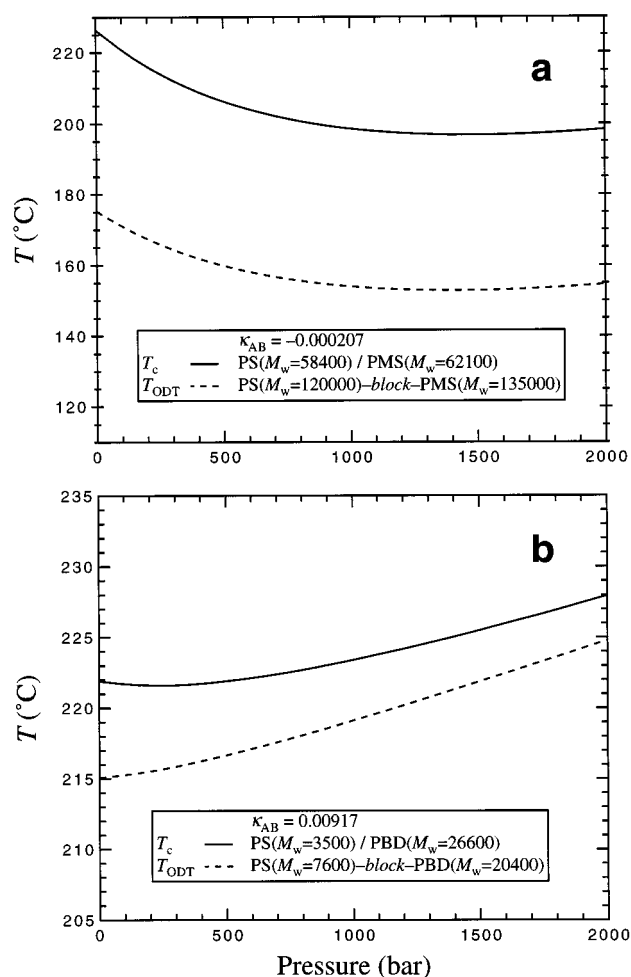


Figure 6. Predicted pressure dependence of critical solution temperature (T_c) for a parent homopolymer blend and that of the order-to-disorder transition temperature (T_{ODT}) for a diblock copolymer melt: (a) Systems containing PS and PMS shown in Figure 2; (b) systems containing PS and PBD shown in Figure 3. These systems exhibit UCST and UCOT behavior. κ_{AB} is independent of pressure.

ture that satisfies $F(q) = 0$. Figure 7b shows the predicted T_{ODT} as functions of pressure and copolymer composition for a PS-PBMA diblock copolymer with $M_w = 99000$. In these systems, miscibility is enhanced by raising the pressure. There is a similar dependence on the pressure between the predicted T_{ODT} for a PS-PBMA diblock copolymer melt and the predicted T_c for a blend of parent homopolymers PS and PBMA.

For systems containing PS and PBMA, the predicted LCST and T_{ODT} associated with LCOT behavior are very sensitive to the pressure. Our theory predicts that for a PS/PBMA blend, LCST rises with increasing pressure at a rate about $+200\text{ }^{\circ}\text{C/kbar}$ that is 1 order of magnitude larger than the measured rates for mixtures of ethylene-vinyl acetate copolymer with a chlorinated polyethylene⁵¹ and for the blend of PSD and PVME⁵² that also exhibit LCST behavior. Similarly, the analysis by Rudolf and Cantow shows that the lattice-fluid theory and the equation-of-state theory by Patterson also predicts a very large pressure dependence of LCST in polymer blends.^{53,54}

IV. Conclusions

The PHSC equation of state^{21–25} is combined with the RPA^{5,14–17} for diblock copolymer melts to represent

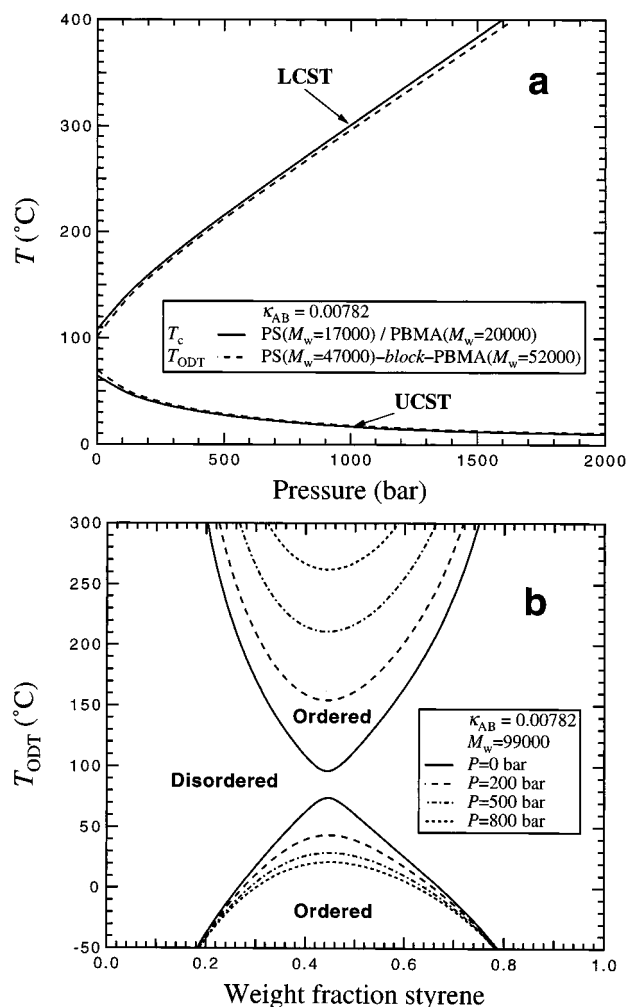


Figure 7. (a) Predicted pressure dependence of critical solution temperature (T_c) for a PS/PBMA blend and that of the order-to-disorder transition temperature (T_{ODT}) for a PS-PBMA diblock copolymer melt shown in Figure 4. (b) Theoretical T_{ODT} as functions of pressure and copolymer composition for a PS-PBMA diblock copolymer with $M_w = 99000$. κ_{AB} is independent of pressure.

UCOT behavior as well as LCOT behavior in compressible diblock copolymer melts. The present model follows closely the RPA for incompressible diblock copolymer solutions by Fredrickson and Leibler¹⁷ based on the Flory-Huggins lattice theory.¹⁸

However, contrary to other models for diblock copolymer melts and solutions,^{12,15,16} we use an equation-of-state theory in continuous space. To demonstrate that off-lattice equation-of-state theories can also be combined with the RPA, a systematic procedure is first presented to combine the RPA with the PHSC equation of state for diblock copolymer melts. This procedure identifies the elements of the interaction matrix in the RPA as the second derivatives of the nonideal Helmholtz energy density with respect to the packing fractions of segments comprising a diblock copolymer.

Theory is compared with experiment for several styrene-based diblock copolymer melts using the binary parameters obtained from the coexistence curve for the binary blend of relevant parent homopolymers. Using the binary parameter obtained in this manner, the order-to-disorder transition temperature of a diblock copolymer melt is predicted. For PS-PMS and PS-PBD diblock copolymer melts that show only UCOT

behavior, the predicted order-to-disorder transition temperatures by the present model are close to those predicted by the RPA combined with the incompressible Flory-Huggins theory.^{15,18,37}

The advantage of the present model lies in its applicability to systems that exhibit LCOT behavior at elevated temperature due to the equation-of-state effect. Our model is also capable of predicting the effect of pressure on the order-to-disorder transition temperatures of diblock copolymer melts.

To demonstrate the present model's capabilities for representing LCOT behavior, our theory is applied to the PS-PBMA diblock copolymer melt that was recently found to show both LCOT and UCOT behaviors.¹⁰⁻¹² The phase behavior of PS-PBMA diblock copolymer melts follows closely that of PS/PBMA homopolymer blends that exhibit both UCST and LCST behaviors in temperature-composition diagrams. Using the same set of binary and equation-of-state parameters, the PHSC equation of state, combined with the RPA, shows semiquantitative agreement with experiment for PS-PBMA diblock copolymer melts as well as for PS/PBMA homopolymer blends.

To illustrate phase separation at elevated temperature, theory is also compared with experiment for systems containing PS and PVME. For PS-PVME diblock copolymer melts, our model predicts a highly asymmetric phase diagram that is similar to the phase diagram of homopolymer blend PS/PVME.

Our model predicts that for a PS-PMS diblock copolymer melt, the theoretical T_{ODT} decreases with increasing pressure. Conversely, theory predicts that for a PS-PBD diblock copolymer melt, T_{ODT} rises with increasing pressure. For a PS-PBMA diblock copolymer melt, the theoretical T_{ODT} associated with LCOT behavior and that associated with UCOT behavior rises and decreases, respectively, with increasing pressure. The predicted T_{ODT} associated with LCOT behavior shows a strong dependence on the pressure that does not agree with limited experimental data concerning the pressure dependence of LCST behavior in polymer blends.

For a given pair of homopolymers, it may be possible to predict the type of phase behavior (e.g., UCST or LCST behavior) by the present theory with $\kappa_{AB} = 0$. However, quantitative predictions of phase-separation temperatures require additional information to determine binary parameter κ_{AB} because phase-separation temperatures in polymer blends and diblock copolymer melts are highly sensitive to κ_{AB} .

Acknowledgment. This work was supported by the Director, Office of Energy Research, Office of Basic Energy Sciences, Chemical Sciences Division of the U.S. Department of Energy under Contract No. DE-AC03-76SF0098. Additional funding was provided by E.I. du Pont de Nemours & Co. (Philadelphia, PA) and Koninklijke Shell (Amsterdam, The Netherlands) and by the donors of the Petroleum Research Fund administered by the American Chemical Society. We thank one of the reviewers for a thorough review of this manuscript.

References and Notes

- (1) Aggarwal, S. L., Ed. *Block Copolymers*; Plenum Press: New York, 1970.
- (2) Noshay, A.; McGrath, J. E. *Block Copolymers: Overview and Critical Survey*; Academic Press: New York, 1977.

- (3) Bates, F. S.; Fredrickson, G. H. *Annu. Rev. Phys. Chem.* **1990**, *41*, 525.
- (4) Matsen, M. W.; Bates, F. S. *Macromolecules* **1996**, *29*, 1091.
- (5) Holyst, R.; Vilgis, T. A. *Makromol. Chem., Theory Simul.* **1996**, *5*, 573.
- (6) Paul, D. R.; Barlow, J. W. *J. Macromol. Sci.-Rev. Macromol. Chem.* **1980**, *C18*, 109.
- (7) Kammer, H. W. *J. Macromol. Sci.-Chem.* **1990**, *A27*, 1713.
- (8) McMaster, L. P. *Macromolecules* **1973**, *6*, 760.
- (9) Patterson, D.; Robard, A. *Macromolecules* **1978**, *11*, 690.
- (10) Russell, T. P.; Karis, T. E.; Gallot, Y.; Mayes, A. M. *Nature* **1994**, *368*, 729.
- (11) Hammouda, B.; Bauer, B. J.; Russell, T. P. *Macromolecules* **1994**, *27*, 2357.
- (12) Karis, T. E.; Russell, T. P.; Gallot, Y.; Mayes, A. M. *Macromolecules* **1995**, *28*, 1129.
- (13) Yeung, C.; Desai, R. C.; Shi, A. C.; Noolandi, J. *Phys. Rev. Lett.* **1994**, *72*, 1834.
- (14) de Gennes, P. G. *Scaling Concepts in Polymer Physics*; Cornell University Press: Ithaca, NY, 1979.
- (15) Leibler, L. *Macromolecules* **1980**, *13*, 1602.
- (16) Fredrickson, G. H.; Leibler, L. *Macromolecules* **1989**, *22*, 1238.
- (17) Akcasu, A. Z.; Klein, R.; Hammouda, B. *Macromolecules* **1993**, *26*, 4136.
- (18) Flory, P. J. *Principles of Polymer Chemistry*; Cornell University Press: Ithaca, NY, 1953.
- (19) Dudowicz, J.; Freed, K. F. *Macromolecules* **1993**, *26*, 213.
- (20) Hashimoto, T.; Hasegawa, H.; Hashimoto, T.; Katayama, H.; Kamigaito, M.; Sawamoto, M.; Imai, M. *Macromolecules* **1997**, *30*, 6819.
- (21) Song, Y.; Lambert, S. M.; Prausnitz, J. M. *Macromolecules* **1994**, *27*, 441.
- (22) Hino, T.; Song, Y.; Prausnitz, J. M. *Macromolecules* **1994**, *27*, 5681.
- (23) Hino, T.; Song, Y.; Prausnitz, J. M. *Macromolecules* **1995**, *28*, 5709.
- (24) Song, Y.; Hino, T.; Lambert, S. M.; Prausnitz, J. M. *Fluid Phase Equilib.* **1996**, *117*, 69.
- (25) Hino, T.; Prausnitz, J. M. *Fluid Phase Equilib.* **1997**, *138*, 105.
- (26) Hino, T.; Prausnitz, J. M. *Liq. Cryst.* **1997**, *22*, 317.
- (27) Tanaka, H.; Sakurai, S.; Hashimoto, T.; Whitmore, M. D. *Polymer* **1992**, *33*, 1006.
- (28) Bidkar, U. R.; Sanchez, I. C. *Macromolecules* **1995**, *28*, 3963.
- (29) Chang, J.; Sandler, S. I. *Mol. Phys.* **1994**, *81*, 735.
- (30) Barlow, J. W. *Polym. Eng. Sci.* **1978**, *18*, 238.
- (31) Quach, A.; Simha, R. *J. Appl. Phys.* **1971**, *42*, 4592.
- (32) Callaghan, T. A.; Paul, D. R. *Macromolecules* **1993**, *26*, 2439.
- (33) Olabisi, O.; Simha, R. *Macromolecules* **1975**, *8*, 206.
- (34) Rodgers, P. A. *J. Appl. Polym. Sci.* **1993**, *48*, 1061.
- (35) Song, Y.; Lambert, S. M.; Prausnitz, J. M. *Ind. Eng. Chem. Res.* **1994**, *33*, 1047.
- (36) Lin, J. L.; Roe, R. J. *Polymer* **1988**, *29*, 1227.
- (37) Kim, J. K.; Han, C. D. *Macromolecules* **1992**, *25*, 271.
- (38) Curran, S.; Kim, J. K.; Han, C. D. *Macromolecules* **1992**, *25*, 4200.
- (39) Fredrickson, G. H.; Helfand, E. *J. Chem. Phys.* **1987**, *87*, 697.
- (40) Zin, W. C.; Roe, R. J. *Macromolecules* **1984**, *17*, 183.
- (41) Roe, R. J.; Zin, W. C. *Macromolecules* **1984**, *17*, 189.
- (42) Roe, R. J.; Zin, W. C. *Macromolecules* **1980**, *13*, 1221.
- (43) Han, C. D.; Kim, J.; Kim, J. K. *Macromolecules* **1989**, *22*, 383.
- (44) Baek, D. M.; Han, C. D.; Kim, J. K. *Polymer* **1992**, *33*, 4821.
- (45) Lipson, J. E. G.; Andrews, S. S. *J. Chem. Phys.* **1992**, *96*, 1426.
- (46) Walsh, D. J.; Dee, G. T.; Halary, J. L.; Ubiche, J. M.; Millequant, M.; Lesec, J.; Monnerie, L. *Macromolecules* **1989**, *22*, 3395.
- (47) Hajduk, D. A.; Gruner, S. M.; Erramilli, S.; Register, R. A.; Fetters, L. J. *Macromolecules* **1996**, *29*, 1473.
- (48) Frielinghaus, H.; Schwahn, D.; Mortensen, K.; Almdal, K.; Springer, T. *Macromolecules* **1996**, *29*, 3263.
- (49) Schwahn, D.; Frielinghaus, H.; Mortensen, K.; Almdal, K. *Phys. Rev. Lett.* **1996**, *77*, 3153.
- (50) Dudowicz, J.; Freed, K. F. *Macromolecules* **1995**, *28*, 6625.
- (51) Walsh, D. J.; Rostami, S. *Macromolecules* **1985**, *18*, 216.
- (52) Janssen, S.; Schwahn, D.; Mortensen, K.; Springer, T. *Macromolecules* **1993**, *26*, 5587.
- (53) Rudolf, B.; Cantow, H. J. *Macromolecules* **1995**, *28*, 6586.
- (54) Rudolf, B.; Cantow, H. J. *Macromolecules* **1995**, *28*, 6595.

MA970796V